RAPID COMMUNICATIONS IN MASS SPECTROMETRY
Rapid Commun. Mass Spectrom. 2010; **24**: 939–957
Published online in Wiley InterScience (www.interscience.wiley.com) DOI: 10.1002/rcm.4465

RCM

Comparison of triple quadrupole, hybrid linear ion trap triple quadrupole, time-of-flight and LTQ-Orbitrap mass spectrometers in drug discovery phase metabolite screening and identification *in vitro* – amitriptyline and verapamil as model compounds

Timo Rousu[1,2], Jukka Herttuainen[3] and Ari Tolonen[1]*

[1]Novamass Ltd., Medipolis Center, Kiviharjuntie 11, 90220 Oulu, Finland
[2]Department of Chemistry, University of Oulu, P.O. Box 3000, 90014 Oulu, Finland
[3]Orion Pharma, P.O. Box 65, 02101 Espoo, Finland

Received 18 December 2009; Revised 14 January 2010; Accepted 15 January 2010

Liquid chromatography in combination with mass spectrometry (LC/MS) is a superior analytical technique for metabolite profiling and identification studies performed in drug discovery and development laboratories. In the early phase of drug discovery the analytical approach should be both time- and cost-effective, thus providing as much data as possible with only one visit to the laboratory, without the need for further experiments. Recent developments in mass spectrometers have created a situation where many different mass spectrometers are available for the task, each with their specific strengths and drawbacks. We compared the metabolite screening properties of four main types of mass spectrometers used in analytical laboratories, considering both the ability to detect the metabolites and provide structural information, as well as the issues related to time consumption in laboratory and thereafter in data processing. Human liver microsomal incubations with amitriptyline and verapamil were used as test samples, and early-phase 'one lab visit only' approaches were used with all instruments. In total, 28 amitriptyline and 69 verapamil metabolites were found and tentatively identified. Time-of-flight mass spectrometry (TOFMS) was the only approach detecting all of them, shown to be the most suitable instrument for elucidating as comprehensive metabolite profile as possible leading also to lowest overall time consumption together with the LTQ-Orbitrap approach. The latter however suffered from lower detection sensitivity and false negatives, and due to slow data acquisition rate required slower chromatography. Approaches with triple quadrupole mass spectrometry (QqQ) and hybrid linear ion trap triple quadrupole mass spectrometry (Q-Trap) provided the highest amount of fragment ion data for structural elucidation, but, in addition to being unable to produce very high-important accurate mass data, they suffered from many false negatives, and especially with the QqQ, from very high overall time consumption. Copyright © 2010 John Wiley & Sons, Ltd.

Most drugs are eliminated from the human body by oxidative and conjugative (phase I & II) biotransformation reactions catalyzed mainly by cytochrome P450 and several conjugative enzymes, of which uridinediphosphate-glucuronosyltransferase (UGT) plays the most important role. The pharmacokinetic properties of drugs are determined to a great extent by metabolic reactions and, therefore, metabolism is often behind bioavailability problems, interindividual variations, metabolic interactions and idiosyncrasies.[1,2] Recently the importance of metabolite profiling studies in the very early phase of drug discovery and development has been stressed, especially by focusing on human metabolism, but profiling metabolites in different toxicity species as well.[3,4] Also the latest FDA guidance encourages that early metabolite profiling is carried out as soon as possible, both *in vitro* and *in vivo*.[5]

Over the past ten years, liquid chromatography in combination with mass spectrometry (LC/MS) has been the preferred tool for the analysis of drugs and their metabolites in both *in vivo* and *in vitro* studies. However, there are several types of mass spectrometers available, each with their specific strengths and drawbacks. Therefore, a decision which one to use for which task also becomes more important, so that as high quality data as possible can be obtained as time and cost effectively as possible.[6] Both data quality and rapid delivery of results play a crucial role in

**Correspondence to*: A. Tolonen, Novamass Ltd., Medipolis Center, Kiviharjuntie 11, 90220 Oulu, Finland.
E-mail: ari.tolonen@novamass.net

RCM

drug discovery and development because the information of metabolic stability, metabolic routes, metabolic interactions and metabolising enzymes and their kinetics is needed for selecting leads and candidates.[1]

To facilitate rapid and time-effective high-quality analysis in drug discovery and early phase development, the analytical approach should provide as much data as possible with only one visit to the laboratory, so that all crucial information would be collected at once, without the need for further experiments. This in turn means that the analytical method should be able to collect data for both molecular ions and fragment ions, at least for the main metabolites, enabling the identification of biotransformations and their approximate sites ('soft-spot') in the parent compound structure. Moreover, this should be provided from test samples with very low parent drug concentrations, as in many cases the new chemical entities (NCEs) under development have low aqueous solubility due to high lipophilicity, limiting the test assay concentrations. In addition to this also information regarding the metabolic stability of the parent compound is often desired from the same experiments, meaning that *in vitro* assays with initial concentration around 1 μM or even less is preferred.

The use of time-of-flight (TOF) or quadrupole time-of-flight (Q-TOF) mass spectrometers in drug metabolite screening is in many case preferred for their high full scan detection sensitivity and mass accuracy coupled to their compatibility for modern fast chromatography by very high data acquisition rate. The detection of all expected and unexpected metabolites in a single run, without the need for preadjustment of detection for certain predicted metabolites and with the possibility of various post-acquisition data filtering and processing options, makes the screening of metabolites both straightforward and cost effective.[7–9] Although some TOF instruments are capable of producing tandem mass spectrometric (MS/MS) information via in-source fragmentation, the advantage of Q-TOF over TOF instruments is in the possibility to obtain more detailed information about the site for the detected biotransformation. The use of both high and low collision energy data acquisition functions in a single LC/MS run provides so called MS^E data, where fragment ion data is acquired for all detected compounds and linked by their retention times.[10] This functionality can be also applied with some limitations to some TOF instruments without a real collision cell, by using two parallel acquisition functions with high and low cone/aperture voltages.

In a LTQ-Orbitrap mass spectrometer, where the high-resolution mass analyzer is usually combined with a linear ion trap, accurate mass measurements are combined with the high trapping capacity and MS^n scan function of the linear ion trap. Therefore, the LTQ-Orbitrap is capable of MS/MS and produces very high accuracy mass data which makes it a useful instrument in identification of biotransformations and their sites as well.[11–13] As a down side, the relatively slow data acquisition rate of the LTQ-Orbitrap makes it incompatible with very fast liquid chromatography, at least if the aim is to analyze several types of data within a single LC/MS run, which is essential for fast high-throughput metabolite screening.

Triple quadrupole (QqQ) mass spectrometers have traditionally been the main work horses of most analytical laboratories. Excellent MS/MS capability of the triple quadrupole instrument is widely used for further elucidation of biotransformation sites in conjunction with accurate mass measurements acquired with different instruments. Even though very high detection sensitivity is obtained in various biological matrices for known analytes in multiple reaction monitoring (MRM) mode, thus being very applicable for quantitative work, the detection sensitivity of QqQ is however rather poor compared to other types of MS instruments when full scan acquisition is used, limiting also the applicability of full scan MS/MS product ion measurement. In addition to product ion scanning, also other full scan data acquisition modes, i.e. neutral loss (NL) and/or precursor ion (PI) scanning functions, have been used for the screening of drug metabolites with QqQ.[14,15] These structure-specific acquisitions result in true positives only if metabolites undergo similar MS/MS fragmentation behaviour as the parent drug, thus many unexpected metabolites may be missed, as well as metabolites with more than one biotransformation site at opposite ends of the molecule. The most commonly used screening method with QqQ is to scan for the neutral loss of phase II conjugated metabolite, e.g. the NL of 176 Da of a glucuronide.[14,16] Moreover, the use of these precursor ion related fragment ion patterns for screening metabolites requires laborious preadjustment of the instrument and usually several LC/MS runs to cover all desired NL and PI acquisition types.

A quite recent major advancement for triple quadrupole technology is the hybrid linear ion trap triple quadrupole (Q-Trap) in which the last quadrupole is replaced by a linear ion trap.[17–19] The ion trap is capable of MS^n as well as high sensitivity scanning, whereas the instrument is also capable of triple quadrupole like collision-induced dissociation (CID) fragment ion production without low mass cut-off and of MRM mode sensitivity. For drug metabolite screening purposes the Q-Trap offers both structure-specific and data-dependent data acquisition modes, of which selected/multiple reaction monitoring (SRM/MRM) triggered enhanced product ion (EPI) MS/MS scanning is most widely used for metabolite screening.[20–22] In addition, approaches utilizing a wide-range scan with the ion trap as a survey scan (EMS, enhanced mass scan), followed by EPI MS/MS (EMS/EPI), have been described.[23]

Depending on what type of mass spectrometer has been used for metabolite screening, a number of different software programs exist for prediction and post-acquisition processing of data.[8,9,24–27] For post-acquisition data processing, the comparison of sample and control chromatograms with these software programs is typically straightforward, revealing the differences in sample and its negative control. All software designed to ease the screening procedure and to increase the throughput must be subjected to careful setup, as with dozens of different parameters and filters the possibility of false negatives is significantly increased.

In this study, we compared the metabolite screening properties of various mass spectrometers widely used in analytical laboratories. Amitriptyline and verapamil human liver microsomal (HLM) incubations *in vitro* were screened

DOI: 10.1002/rcm

for metabolites with TOF, QqQ and Q-Trap mass spectrometers coupled to ultra-performance liquid chromatographic (UPLC), and amitriptyline samples were also screened with a LTQ-Orbitrap. Amitriptyline and verapamil were selected as test compounds in this study as both of them are known to undergo extensive oxidative metabolism and have been widely studied by LC/MS.[28–31] These two model compounds also have distinctive differences: (a) amitriptyline forms through very comprehensive fragmentation ten major fragment ions in CID, whereas verapamil forms only four major fragment ions; and (b) amitriptyline serves as a model compound with quite simple expected metabolism, whereas verapamil has several expected biotransformation sites, producing a very high number of metabolites formed via combinations of several reactions in various sites of the parent compound structure. The number of major fragment ions for the parent compound has naturally a large impact on the number of NL/PI transition reactions or ions that can be utilized in targeted metabolite analysis. The aim was to use an approach suitable for tentative discovery/early development phase metabolite screening meaning as few runs per sample as possible, and that all data, including precursor and fragment ion data, should be acquired with only one visit to the laboratory without the need for additional experiments.

EXPERIMENTAL

Reagents and materials

HPLC grade acetonitrile (LiChrosolv GG) and dimethyl sulfoxide (DMSO) (SeccoSolv) were purchased from Merck (Darmstadt, Germany). Acetic acid was purchased from BDH Laboratory Supplies (Poole, UK). Laboratory water was distilled and purified with a Direct-Q water purifier (Millipore, Molsheim, France). Both of the test compounds, NADPH and UDPGA were all purchased from Sigma-Aldrich (Helsinki, Finland).

Microsomal incubations and sample preparation

Pooled liver microsomes containing 20 mg protein/mL were obtained from BD Biosciences Discovery Labware (Woburn, MA, USA). Human microsomal pool (Lot#99268) consisted of liver samples from 30 donors of both genders. The basic incubation mixture of 250 μL in volume consisted of the following components: 0.5 mg of microsomal protein per mL, substrate in DMSO, 1 mM NADPH and 1 mM UDPGA. The substrate concentration used was 10 μM. Two parallel incubations, one with cofactors and one without, were employed. The final amount of DMSO in the incubation was 1% (v/v). Each reaction mixture was preincubated for 2 min at 37°C in a shaking incubator block (Eppendorf Thermomixer 5436, Hamburg, Germany). The incubation reactions were started by addition of NADPH and UDPGA. After an incubation period of 0 or 60 min, a 100 μL sample was collected and the reaction was terminated by adding an equal volume of ice-cold acetonitrile. Control incubations were performed without the test compounds. Samples were subsequently cooled in an ice bath and the tubes were stored at −18°C until analysis. The incubation samples were thawed at room temperature, shaken and centrifuged for 10 min at 16100 *g* (Eppendorf 5415D, Eppendorf AG, Hamburg, Germany) and pipetted to Maximum Recovery vials (Waters Corp., Milford, MA, USA).

Liquid chromatography

In combination with triple quadrupole, hybrid linear ion trap triple quadrupole and time-of-flight mass spectrometry, a Waters Acquity ultra-performance liquid chromatographic (UPLC) system (Waters Corp.) with an autosampler, a vacuum degasser and a column oven was used. A Waters BEH ShieldRP18 column (2.1 × 50 mm, 1.7 μm) was used together with an on-line filter. The eluents were 0.1% acetic acid (A, pH 3.2) and acetonitrile (B). A linear gradient elution with profile 5% – 20% – 85% – 85% B in 0 – 5 – 6 – 7 min was applied, followed by column equilibration. The flow rate was 0.5 mL/min and the column oven temperature was 35°C. A 4 μL injection volume was used. The first 0.6 min of the run was directed to waste by using a divert valve to decrease the ion source contamination from early eluting matrix constituents. The UPLC system was operated under MassLynx 4.1 software (with TOFMS and QqQ) or Analyst 1.4.2 software (with Q-Trap).

With LTQ-Orbitrap mass spectrometry the chromatographic system consisted of a Thermo Accela liquid chromatograph (Thermo-Fischer, San Jose, CA, USA) with a Thermo Hypersil Gold C18 column (2.1 × 50 mm, 3.0 μm). The same eluents as described above were used at a flow rate of 0.2 mL/min and a gradient profile of 5% – 20% – 85% – 85% B in 0 – 9 – 11 – 13 min, followed by column equilibration. An ambient column oven temperature was used, and the injection volume was 4 μL. The LC system was operated under Xcalibur 2.0.7 software.

TOF experiments

Data was acquired with a Waters LCT Premier XE time-of-flight (TOF) mass spectrometer (Waters Corp.) equipped with a LockSpray electrospray ionization (ESI) source. The positive ionization mode of ESI was used with a capillary voltage of 2800 V and a cone voltage of 40 V. Two parallel data acquisition functions were used, with aperture voltages of 5 V (for molecular ions) and 50 V (for fragmentation). An acquisition time (scan time) of 100 ms per data point was used leading to a total cycle time of 200 ms. Lock mass data was acquired in every 10th scan. The mass range of *m/z* 150–750 was acquired, using a W-mode flight tube optics at resolution of 12 000 (FWHM) and dynamic range enhancement (DRE) option. Desolvation temperature used was 350°C and source temperature was 150°C. Nitrogen was used both as desolvation and as nebulizer gas. Leucine enkephalin was used as a lock mass compound ($[M+H]^+$ *m/z* 556.2771) for accurate mass measurements and was infused into the LockSpray ion source via a separate ionization probe using a syringe pump. The mass spectrometer was operated under MassLynx 4.1 software. Metabolites were mined from the data by using the MetaboLynx XS subroutine of the MassLynx software, employing the dealkylation tool and 'chemically intelligent' (structure based) mass defect filtering (MDF) with a 40 mDa tolerance window. The real positives (metabolites) and their identifications were confirmed from the data manually. Metabolites with signal-to-noise (S/N)

DOI: 10.1002/rcm

ratio >3 in the ion chromatogram, measured accurate mass within 3 mDa from the calculated mass and signals missing from negative controls were considered as real positives.

Triple quadrupole experiments

Data was acquired with a Waters Quattro Premier triple quadrupole mass spectrometer (Waters Corp.) equipped with a Z-spray ESI source. The positive ionization mode of ESI was used with a capillary, extractor and RF lens voltages of 2800 V, 3 V and 0.2 V, respectively. With amitriptyline a cone voltage of 32 V was used and with verapamil the cone voltage was set to 40 V. With amitriptyline, the ten most abundant fragment ions were selected for precursor ion (PI) scan/neutral loss (NL) scan functions assuming similar fragmentation behaviour for the metabolites as for the parent drug, whereas for verapamil the four most abundant fragment ions were selected. The used PI/NL scan functions with corresponding collision energies for both of the compounds are summarized in Table 1. All NL/PI experiments were run using only one PI or NL scan/transition at a time, i.e. in total 21 runs/sample for amitriptyline and 9 runs/sample for verapamil were acquired. Scan times used were 0.3 s. Collision gas was argon with a CID gas cell pressure of 3.90×10^{-3} mbar. Desolvation temperature was 350°C and source temperature was 150°C. Nitrogen was used both as desolvation and as nebulizer gas. The mass spectrometer was operated under MassLynx 4.1 software. Metabolites were mined from the data manually, by looking directly for visually detectable peaks in LC/MS/MS chromatograms, and by searching ion chromatograms for the common predicted metabolites. Metabolites with S/N ratio >3 in ion chromatograms extracted from PI or NL data and signals missing from negative controls were considered as real positives.

Hybrid linear ion trap triple quadrupole experiments

LC/MS/MS data was acquired with a Applied Biosystems/MDS SCIEX 4000 QTrap® triple quadrupole/linear ion trap (QqQ_{LIT}) mass spectrometer (Applied Biosystems, Foster City, CA, USA) equipped with a TurboIonSpray® interface operating in the positive ESI mode. A SRM-ER-EPI approach was used in which SRM functions as survey scan and exploits the triple quadrupole mode of the instrument. Information-dependent acquisition (IDA) methods link the survey scan to ER (Enhanced Resolution Scan) and EPI (Enhanced Product Ion Scan) utilizing the linear ion trap mode of the instrument. Instrument parameters for SRM mode were optimized by infusing each analyte dissolved in methanol/water/formic acid (50:50:0.1). Parameters for amitriptyline were declustering potential (DP) 50, EP 10, collision energy (CE) 25, CXP 18 and for verapamil DP 70, EP 10, CE 45, CXP 20. SRM parameters optimized for amitriptyline and verapamil were used as a basis when generating the SRM transitions for the metabolites, assuming fragmentation behaviour of the metabolites and the parent drug to be similar. Predicted SRM transitions used for the metabolite screening of amitriptyline and verapamil samples are presented in Table 1. The scan time for each SRM transition was 5 ms. ER and EPI acquisitions were triggered when ions detected with SRM exceeded 500 counts per second (cps). ER scanning was performed at step size 0.03 amu, scan rate 250 amu/s, 2 ms pause between mass ranges and Q0 trapping on. EPI scanning was performed at step size 0.08 amu, scan rate 1000 amu/s and 2 ms pause between mass ranges. Dynamic fill time of the trap was applied in both ER and EPI. In the EPI scan, DP and CE were as follows: amitriptyline 50 and 30; verapamil 70 and 40. Total cycle time of the amitriptyline method was 1.19 s and of the verapamil method 1.44 s. Ion source conditions for both amitriptyline and verapamil were set as follows: CUR = 20, CAD = 5, IS = 5000, TEM = 450°C, GS1 = 50 and GS2 = 50. Samples were also analyzed with a full scan method (EMS-ER-EPI) using mass range 100–600 amu for amitriptyline and 200–700 amu for verapamil. EMS scanning was performed at step size 0.08 amu, scan rate 1000 amu/s, 2 ms pause between mass ranges and with dynamic fill time on. ER and EPI parameters in the full scan methods were identical to the SRM-ER-EPI method described above. Total cycle time of the amitriptyline method was 1.71 s and of the verapamil method 1.80 s. Nitrogen was used as the nebulizer and auxiliary gas. The mass spectrometer was operated under Analyst® (version 1.4.2) software. Metabolites were mined from the data manually, by looking directly for visually detectable peaks in LC/MS/MS chromatograms. Metabolites with S/N ratio >3 in SRM chromatograms, ER spectrum confirming the metabolite found with SRM, EPI fragment data fitting to study compound related structures,

Table 1. The NL/PI and SRM reactions used with the triple quadrupole and Q-Trap instruments

PI/NL functions for amitriptyline and metabolites; parents for *m/z*/neutral loss of Da (collision energy eV)	233/45 (16), 218/60 (24), 205/73 (24), 191/87 (22), 155/123 (24), 129/149 (24), 117/161 (22), 105/173 (24), 91/187 (24), 84/194 (24), NL of 176 (25) for glucuronides
PI/NL functions for verapamil and metabolites; parents for *m/z*/neutral loss of Da (collision energy eV)	303/152 (24), 260/195 (32), 165/290 (26), 150/305 (38), NL of 176 (25) for glucuronides
SRM transitions for amitriptyline and metabolites; *m/z*>*m/z*	278>191, 294>207, 294>191, 294>100, 310>223, 310>207, 310>116, 264>191, 264>70, 250>191, 250>56, 270>189, 276>82, 454>278, 452>276, 470>294, 292>205, 292>98, 296>209, 298>225, 298>70, 312>225, 468>292, 280>207, 280>89, 440>264
SRM transitions for verapamil and metabolites; *m/z*>*m/z*	455>303, 441>151, 441>165, 441>289, 441>303, 617>441, 457>165, 457>167, 457>303, 457>305, 633>457, 427>137, 427>151, 427>165, 427>275, 427>289, 427>303, 603>427, 443>151, 443>289, 471>165, 471>181, 471>303, 471>319, 631>455, 469>165, 469>303, 647>471, 291>248, 277>234, 307>264, 307>307, 453>277

DOI: 10.1002/rcm

and signals missing from negative controls were considered as real positives.

LTQ-Orbitrap experiments

Data was acquired using a LTQ-Orbitrap mass spectrometer (Thermo Fisher Scientific, Bremen, Germany). An approach with high-resolution (15 000 FWHM) scan at mass range *m/z* 100–750 as a survey scan was utilized, and parallel low-resolution MS/MS data using the ion trap function was acquired data-dependently for the two most intense ions in each high-resolution survey scan (unit resolution). CID was conducted with an isolation width of 5 Da, normalized collision energy of 35, activation q of 0.25 and an activation time of 30 ms. Dynamic exclusion was conducted by utilizing a repeat count of one prior to exclusion. Ions with unassigned or multiple charge states were excluded from CID, as well as known background ions. Total scan cycle time was about 1 s, formed from 0.4 s high resolution scan and two 0.25 s data-dependent MS/MS scans. The source parameters of 5000 V for capillary voltage, 275°C of capillary temperature, sheath gas (nitrogen) flow of 8 units and tube lens voltage of 90 V were used. External calibration of the instrument was conducted just before experiments. The instrument was controlled by Xcalibur 2.0.7 software. The data was processed both manually for expected metabolites, using ion chromatograms with 20 mDa window, and by using Thermo MetWorks software with MDF with 80 mDa tolerance window.

Data processing methods and set criteria for metabolite hits

The actual samples were compared with the control samples without the study compound. Positive hits were also compared manually with the 0 min samples to distinguish them from possible impurities present with the study compound. TOFMS data was mined using a MetaboLynx XS subroutine of the MassLynx-software, the expected metabolite list included the expected phase I and phase II biotransformations for amitriptyline and verapamil to undergo in a human liver microsomal incubation with the used cofactors, i.e. hydroxylation, dihydroxylation, demethylation, didemethylation, hydrogenation, dehydrogenation and glucuronide conjugation, as well as all possible combinations of the abovementioned reactions (combinations created by the software itself). The dealkylation tool of the software was enabled with a mass cut-off of 70 Da allowing it to break two bonds. The mass defect filter was enabled with a tolerance of 40 mDa. Expected mass chromatograms were created with a mass window of 0.05 Da. For unexpected metabolites full acquisition mass range chromatograms were created with a 1 Da window. The peak detection threshold for absolute peak area was set to slightly overcome the normal noise level with the instrument.

The precursor ion scan and neutral loss scan data and the SRM/EPI-MS data obtained from triple quadrupole instruments were processed manually. In the case of NL and PI data, 20 different predefined extracted ion chromatograms with amitriptyline and 42 with verapamil were used to cover possible biotransformations. The LTQ-Orbitrap data was processed both manually for expected metabolites, using ion chromatograms with a 20 mDa window, and by using Thermo MetWorks software. The same expected metabolites list as with MetaboLynx (see above) was used and MDF was used with 80 mDa tolerance window.

With data from all instrument types, a detectable peak (S/N ratio >3) in the sample (60 min incubation) that was not present in the control samples (incubation without the study compound and the 0 min sample with the study compound) was considered as a positive hit. In addition, an accurate mass criteria with <3 mDa difference to the calculated mass value was set for TOFMS and the LTQ-Orbitrap. Also adequate fragment ion data confirming the metabolite to be in a similar structural family as the parent compound was an additional criterion for both types of triple quadrupole instruments. All positive hits were also evaluated manually to exclude them from false positives.

Data from TOFMS and both types of triple quadrupole instrument approaches were processed and mined for metabolites as individual studies so that no information of the found metabolites with one instrument was used with the other instruments, thus providing the comparison of metabolite screening possibilities of these instruments to be more informative and directly comparable. When mining the LTQ-Orbitrap data, the results from TOFMS were used as a basis, to avoid the features and suitability of the used software (MetaboLynx or MetWorks) having too large an impact on the results between these two instrument types.

RESULTS AND DISCUSSION

Metabolite hits and detection sensitivity with different mass spectrometers

In total, 28 confirmed amitriptyline metabolites were found and tentatively identified from 60 min *in vitro* HLM incubations. All of these were found by the TOFMS approach. The same samples analyzed with Q-Trap, QqQ or LTQ-Orbitrap resulted in 11, 10 and 13 metabolite hits, respectively. Ten of the Q-Trap metabolites were detected using the SRM-ER-EPI-approach, and one additional metabolite was found by the acquisition of EMS-ER-EPI data. Verapamil incubations resulted in 69, 21 and 24 metabolite hits when analyzed with TOF, Q-Trap or QqQ, respectively. No data with the LTQ-Orbitrap was acquired for verapamil. Twenty of the verapamil Q-Trap metabolites were detected using the SRM-ER-EPI-approach, and again one additional metabolite was found by the acquisition of EMS-ER-EPI data. Metabolite hits with various instruments for both of the compounds are collected in Tables 2 and 3, including identifications of biotransformations (and their sites where applicable). Detailed LC/MS data for all detected metabolites are presented in Tables 4 and 5, including accurate mass (in-source) fragment ion data from TOFMS and all low-resolution fragment ion data from the other MS instruments. Metabolic schemes with structures of the metabolites for both compounds are presented in Figs. 1 and 2.

The number of hits correlated well with the assumption that the detection sensitivity is clearly higher when TOFMS is used instead of QqQ in PI or NL scanning mode, and that certain unexpected metabolites are missed by the PI/NL or SRM-EPI approach, as those are limited to only predefined

DOI: 10.1002/rcm

RCM

Table 2. The number of metabolite hits with different MS instruments for amitriptyline

Metabolite	Biotransformation/Data processing	Hits TOF MetaboLynx + manual	Hits QTrap manual	Hits QqQ manual	Hits Orbitrap MetWorks + manual
Parent	Unchanged	x	x	x	x
M1	N-Demethylation	x	x	x	x
M2	2 × N-Demethylation	x	x	x	x
M3	Hydroxylation to ethylene bridge in central ring	x	x	x	x
M4	Hydroxylation	x			
M5	Hydroxylation to ethylene bridge in central ring	x	x	x	x
M6	Aromatic hydroxylation	x	x	x	x
M7	Aromatic hydroxylation	x	x		x
M8	Aromatic hydroxylation	x	x	x	x
M9	Hydroxylation	x			x
M10	Hydroxylation to area between N and central ring	x	x	x	x
M11	Methyl hydroxylation	x	x	x	x
M12	2 × Hydroxylation/N-Oxidation	x			
M13	2 × Hydroxylation/N-Oxidation	x			
M14	2 × Hydroxylation/N-Oxidation	x			
M15	2 × Hydroxylation/N-Oxidation	x			
M16	2 × Hydroxylation/N-Oxidation	x			
M17	Hydroxylation + N-Demethylation	x			
M18	Hydroxylation + N-Demethylation	x			
M19	Hydroxylation + N-Demethylation	x			
M20	Hydroxylation + N-Demethylation	x			
M21	Hydroxylation + N-Demethylation	x			
M22	Hydroxylation + N-Demethylation	x			
M23	2 × Hydroxylation + N-Demethylation	x			
M24	Hydroxylation + Dehydrogenation (oxo to ethylene bridge)	x	x	x	x
M25	Hydroxylation + Dehydrogenation	x			x
M26	Hydroxylation + Dehydrogenation + N-Demethylation	x			
M27	N-Glucuronide conjugation	x		x	x
M28	Hydroxylation + Glucuronide conjugation	x	x		

Table 3. The number of metabolite hits with different MS instruments for verapamil

Metabolite	Biotransformation/Data processing	Hits TOF MetaboLynx + manual	Hits QTrap manual	Hits QqQ manual
Parent	Unchanged	x	x	x
M1	O-Demethylation (to ring A)	x	x	x
M2	O-Demethylation (to ring A)	x	x	x
M3	O-Demethylation (to ring B)	x	x	x
M4	N-Demethylation	x	x	x
M5	2 × Demethylation (both to ring A or one to ring A and N-Demethylation)	x	x	x
M6	2 × Demethylation (both to ring A or one to ring A and N-Demethylation)	x	x	x
M7	2 × Demethylation	x		
M8	3 × Demethylation	x		
M9	Hydroxylation	x		
M10	Hydroxylation/N-oxidation to C17H25N2O2 area	x	x	x
M11	Hydroxylation/N-oxidation to C17H25N2O2 area	x	x	x
M12	Hydroxylation/N-oxidation	x		
M13	Hydroxylation/N-oxidation	x		
M14	Hydroxylation (to ring B or carbon next to it)	x	x	
M15	Hydroxylation/N-oxidation	x		
M16	Hydroxylation (to ring B or carbon next to it)	x	x	x
M17	2 × Hydroxylation (to C10H12O2 area)	x		x
M18	3 × Hydroxylation/N-oxidation	x		
M19	3 × Hydroxylation/N-oxidation	x		
M20	3 × Hydroxylation/N-oxidation	x		
M21	Hydroxylation to isopropyl + N-Demethylation	x	x	x

(*Continues*)

DOI: 10.1002/rcm

Table 3. (Continued)

Metabolite	Biotransformation/Data processing	Hits TOF MetaboLynx + manual	Hits QTrap manual	Hits QqQ manual
M22	Methyl hydroxylation + Demethylation	x		
M23	Methyl hydroxylation + Demethylation (not in ring B)	x	x	
M24	Hydroxylation + Demethylation to C17H25N2O2 area	x	x	x
M25	Hydroxylation + Demethylation	x		
M26	Hydroxylation + Demethylation	x		
M27	Hydroxylation to isopropyl + O-Demethylation (to ring B)	x		
M28	Hydroxylation to C10H12O2 area + N-Demethylation	x	x	x
M29	Hydroxylation + 2 × Demethylation	x		
M30	Hydroxylation + 2 × Demethylation	x		
M31	Hydroxylation + 2 × Demethylation	x		
M32	Hydroxylation + 2 × Demethylation	x		
M33	Hydroxylation + 2 × Demethylation	x		
M34	N-Dealkylation by loss of C10H12O2	x	x	x
M35	N-Dealkylation + O-Demethylation	x		
M36	N-Dealkylation + O-Demethylation	x		
M37	N-Dealkylation + N-Demethylation	x	x	x
M38	N-Dealkylation + 2 × Demethylation	x		
M39	N-Dealkylation + Demethylation + Hydroxylation	x		
M40	N-Demethylation + Dehydrogenation	x		x
M41	Demethylation + Dehydrogenation	x		
M42	Demethylation + Dehydrogenation	x		
M43	Demethylation + 2 × Dehydrogenation	x		
M44	2 × Demethylation + Dehydrogenation	x		
M45	2 × Demethylation + Dehydrogenation	x		
M46	2 × Demethylation + Dehydrogenation	x		
M47	2 × Demethylation + Dehydrogenation	x		
M48	Hydroxylation + Demethylation + Dehydrogenation	x		
M49	Hydroxylation + Demethylation + Dehydrogenation	x		
M50	Hydroxylation + Demethylation + Dehydrogenation to C17H25N2O2 area	x		x
M51	Hydroxylation + Demethylation + Hydrogenation	x		
M52	Cleavage of C17H25N2O2 + Hydroxylation	x		
M53	Glucuronide conjugation	x	x	x
M54	O-Demethylation (to ring A) + Glucuronide conjugation	x	x	x
M55	O-Demethylation (to ring B) + Glucuronide conjugation	x	x	x
M56	Demethylation + Glucuronide conjugation	x	x	x
M57	2 × Demethylation + Glucuronide conjugation	x		
M58	2 × Demethylation + Glucuronide conjugation	x		
M59	2 × Demethylation (both to ring A or one to ring A and N-Demethylation) + Glucuronide conjugation	x	x	x
M60	Hydroxylation + Glucuronide conjugation	x		x
M61	Hydroxylation + Demethylation + Glucuronide conjugation	x		
M62	Hydroxylation + Demethylation + Glucuronide conjugation	x		
M63	Hydroxylation + Demethylation + Glucuronide conjugation	x		
M64	Hydroxylation + Demethylation + Glucuronide conjugation	x		
M65	Hydroxylation + Demethylation + Glucuronide conjugation	x		x
M66	Hydroxylation + Demethylation + Glucuronide conjugation	x		
M67	Hydroxylation + 2 × Demethylation + Glucuronide conjugation	x		
M68	2 × Demethylation + Dehydrogenation + Glucuronide conjugation	x		
M69	N-Dealkylation + Demethylation + Glucuronide conjugation	x		

expected metabolites, or metabolites that undergo similar predefined fragmentation reactions. The main metabolites were detected with all MS approaches. It is also worth mentioning that as the Q-Trap is also a triple quadrupole instrument with fully functional NL and PI scan modes, it must be assumed that all metabolites detected here with the traditional triple quadrupole instrument would have been detected also with the Q-Trap by using the same NL/PI scan approach. When comparing the hit rate with the triple quadrupole and the Q-Trap instruments, it is also worth noticing that a higher number of PI/NL reactions were used with the triple quadrupole than fragmentation reactions for predicting the used SRM transitions with the Q-Trap. Thus, if the number of PI/NL reactions with triple quadrupole instruments had been decreased so that only one LC/MS run had been acquired (as with Q-Trap), the hit rate would have been probably clearly decreased to be less than that with the Q-Trap.

An example of the detection sensitivities of the four different mass spectrometers used in this study is illustrated in Fig. 3, in which extracted ion chromatograms (XICs) of the didemethylated metabolite of amitriptyline (M2) are shown. On the top is a XIC from LTQ-Orbitrap data (Fig. 3(A)), the next XIC being from Q-Trap data (Fig. 3(B)) and the following two XICs being from QqQ (Fig. 3(C)) and TOF (Fig. 3(D)) data, respectively. The figure shows that S/N ratio with

DOI: 10.1002/rcm

Table 4. Accurate mass and fragment ion data measured for amitriptyline and its metabolites

	Metabolite Name	Ion	*m/z* Calc	mDa TOF	mDa orbitrap	RT min	%	Fragment ions from QqQ, Orbitrap and QTrap
Parent	Amitriptyline	$[M+H]^+$	278.1909	0.2	0.6	5.43		QqQ: 278, 264, 233, 218, 205, 191, 155, 129, 117, 105, 91, 84
	loss of C2H7N	$[C18H17]^+$	233.1330	−0.1				Orbitrap: 233, 205, 191, 155, 117, 105, 91
	loss of C3H10N	$[C17H14]^+$	218.1096	0.7				QTrap: 278, 233, 218, 205, 203, 191, 178, 155, 153, 141, 129,
	loss of C4H11N	$[C16H13]^+$	205.1017	2.3				117, 115, 105, 91, 84, 82, 79
	loss of C5H13N	$[C15H11]^+$	191.0861	1.7				
	loss of C6H13N	$[C14H11]^+$	179.0861	1.3				
	loss of C8H13N	$[C12H11]^+$	155.0861	0.2				
M1	N-Demethylation	$[M+H]^+$	264.1752	0.2	0.4	5.34	65.6	QqQ: 264, 233, 218, 205, 204, 191, 177, 155, 145, 129, 117, 115,
	loss of CH5N	$[C18H17]^+$	233.1330	0.6				105, 103, 91, 70
	loss of C2H8N	$[C17H14]^+$	218.1096	2.0				Orbitrap: 233, 205, 191, 155, 117, 105, 91
	loss of C3H9N	$[C16H13]^+$	205.1017	2.3				QTrap: 264, 233, 218, 205, 203, 191, 178, 155, 153, 117, 115, 105, 91
	loss of C4H11N	$[C15H11]^+$	191.0861	3.5				
	loss of C7H11N	$[C12H11]^+$	155.0861	0.7				
M2	2 × N-Demethylation	$[M+H]^+$	250.1596	0.5	0.8	5.16	1.2	QqQ: 250, 233, 191, 155, 105, 91
	loss of H3N	$[C18H17]^+$	233.1330	0.3				QTrap: 250, 233, 218, 205, 191, 178, 155, 105, 91
	loss of CH6N	$[C17H14]^+$	218.1096	0.3				
	loss of C2H7N	$[C16H13]^+$	205.1017	0.1				
M3	Hydroxylation to ethylene bridge in central ring	$[M+H]^+$	294.1858	0.4	0.6	2.57	7.7	QqQ: 294, 276, 249, 231, 205, 203, 191, 105, 84
	loss of H2O	$[C20H22N]^+$	276.1752	0.5				Orbitrap: 276, 231
	losses of C2H7N and H2O	$[C18H15]^+$	231.1174	0.4				QTrap: 294, 276, 231, 229, 216, 215, 205, 203, 191, 179, 153, 84
	losses of C3H10N and H2O	$[C17H12]^+$	216.0939	1.2				
	loss of C4H9N and H2O	$[C16H13]^+$	205.1017	0.7				
	loss of C5H11N and H2O	$[C15H11]^+$	191.0861	0.4				
M4	Hydroxylation	$[M+H]^+$	294.1858	−0.2		3.27	0.3	
M5	Hydroxylation to ethylene bridge in central ring	$[M+H]^+$	294.1858	0.6	0.6	3.48	2.2	QqQ: 294, 276, 249, 205, 191
	loss of H2O	$[C20H22N]^+$	276.1752	−1.6				Orbitrap: 276
	losses of C2H7N and H2O	$[C18H15]^+$	231.1174	1.4				QTrap: 294, 276, 231, 229, 218, 215, 205, 203, 191, 178, 153, 117, 91, 84
	losses of C3H10N and H2O	$[C17H12]^+$	216.0939	0.0				
	loss of C4H11NO	$[C16H13]^+$	205.1017	−0.2				
M6	Aromatic hydroxylation	$[M+H]^+$	294.1858	2.1	0.0	3.62	0.7	QqQ: 294, 249, 221, 171, 105, 91
	loss of C2H7N	$[C18H17O]^+$	249.1279	0.7				QTrap: 294, 249, 234, 231, 221, 207, 194, 179, 157, 155, 133, 121, 107, 105
M7	Aromatic hydroxylation	$[M+H]^+$	294.1858	−0.1	0.5	3.71	0.3	QTrap: 294, 249, 207, 155, 121, 84
M8	Aromatic hydroxylation	$[M+H]^+$	294.1858	0.5	0.5	4.16	0.3	QqQ: 294, 249 QTrap: 294, 249, 207, 117, 107, 91
M9	Hydroxylation	$[M+H]^+$	294.1858	0.3	0.1	4.48	0.5	
M10	Hydroxylation to area between nitrogen and central ring	$[M+H]^+$	294.1858	0.4	0.6	4.96	5.1	QqQ: 294, 249, 205
M11	Methyl hydroxylation	$[M+H]^+$	294.1858	−0.2	0.5	5.60	8.2	QqQ: 294, 278, 264, 233, 218, 205, 191, 155, 145, 129, 117, 105, 91
	loss of C2H7NO	$[C18H17]^+$	233.1330	−0.2				Orbitrap: 233, 191, 155, 117, 105, 91
	loss of C3H10NO	$[C17H14]^+$	218.1096	0.0				QTrap: 294, 233, 218, 212, 203, 191, 155, 117, 91
	loss of C4H11NO	$[C16H13]^+$	205.1017	1.0				
	loss of C5H13NO	$[C15H11]^+$	191.0861	1.0				

DOI: 10.1002/rcm

RCM

M12	2 × Hydroxylation/N-Oxidation	$[M+H]^+$	310.1807	−0.5		2.35	0.2	
	loss of CH2	$[C19H22NO2]^+$	296.1651	1.5				
M13	2 × Hydroxylation/N-Oxidation	$[M+H]^+$	310.1807	0.2		3.06	0.2	
M14	2 × Hydroxylation/N-Oxidation	$[M+H]^+$	310.1807	2.3		3.92	0.1	
M15	2 × Hydroxylation/N-Oxidation	$[M+H]^+$	310.1807	1.3		5.10	0.1	
M16	2 × Hydroxylation/N-Oxidation	$[M+H]^+$	310.1807	2.0		5.54	0.1	
M17	Hydroxylation + N-Demethylation	$[M+H]^+$	280.1701	−0.2		2.50	1.1	
	loss of H2O	$[C19H20N]^+$	262.1596	0.5				
	losses of C2H8N and H2O	$[C17H12]^+$	216.0939	0.5				
M18	Hydroxylation + N-Demethylation	$[M+H]^+$	280.1701	−2.7		3.23	0.1	
M19	Hydroxylation + N-Demethylation	$[M+H]^+$	280.1701	−0.7		3.38	0.2	
M20	Hydroxylation + N-Demethylation	$[M+H]^+$	280.1701	−0.1		3.50	0.1	
M21	Hydroxylation + N-Demethylation	$[M+H]^+$	280.1701	0.5		4.34	0.1	
M22	Hydroxylation + N-Demethylation	$[M+H]^+$	280.1701	0.3		4.81	1.8	
	loss of C2H7NO	$[C17H15]^+$	219.1174	−0.4				
M23	2 × Hydroxylation + N-Demethylation	$[M+H]^+$	296.1651	−2.1		2.27	0.1	
M24	Hydroxylation + Dehydrogenation (oxo to ethylene bridge)	$[M+H]^+$	292.1701	0.4	0.1	3.66	1.2	QqQ: 292, 232, 219, 205, 191, 145, 91, 84
	losses of C2H7N and H2O	$[C18H13]^+$	229.1017	1.1				QTrap: 292, 229, 219, 203, 191, 178, 91, 84
	loss of C5H9N and H2O	$[C15H11]^+$	191.0861	0.3				
M25	Hydroxylation + Dehydrogenation	$[M+H]^+$	292.1701	−0.1	0.2	3.88	0.3	
M26	Hydroxylation + Dehydrogenation + N-Demethylation	$[M+H]^+$	278.1545	−0.8		3.59	0.3	
M27	N-Glucuronide conjugation	$[M+H]^+$	454.2230	0.1	0.6	5.66	2.1	QqQ: 454, 278, 233, 218, 205, 191, 155, 129, 117, 105, 91
	loss of C6H8O6	$[C20H24N]^+$	278.1909	0.0				
	loss of C8H15NO6	$[C18H17]^+$	233.1330	0.4				
M28	Hydroxylation + Glucuronide conjugation	$[M+H]^+$	470.2179	−0.1		3.04	0.3	QTrap: 470, 294, 276, 231, 191, 184

mDa = difference between calculated and obtained accurate mass

% = share of total combined metabolite peak areas from TOFMS data assuming similar MS response of the metabolites

DOI: 10.1002/rcm

Table 5. Accurate mass and fragment ion data measured for verapamil and its metabolites

	Metabolite name	Ion	*m/z* Calc.	mDa TOF	RT (min)	%	Fragment ions from QqQ and QTrap
Parent	Verapamil	$[M+H]^+$	455.2910	−0.2	5.58		QqQ: 455, 441, 303, 289, 260, 246, 165, 151, 150, 136
	loss of C9H12O2	$[C18H27N2O2]^+$	303.2073	0.0			
	loss of C11H17NO2	$[C16H22NO2]^+$	260.1651	0.6			QTrap: 455, 303, 260, 243, 218, 177, 165, 150, 135
	loss of C17H26N2O2	$[C10H13O2]^+$	165.0916	0.2			
M1	O-Demethylation (to ring A)	$[M+H]^+$	441.2753	−0.2	5.11	1.8	QqQ: 441, 427, 303, 289, 260, 165, 151, 150
	loss of C16H24N2O2	$[C10H13O2]^+$	165.0916	1.1			QTrap: 441
M2	O-Demethylation (to ring A)	$[M+H]^+$	441.2753	2.1	5.26	0.8	QqQ: 441, 165, 150
	loss of C9H12O2	$[C17H25N2O2]^+$	289.1916	2.0			QTrap: 441, 289, 246, 231, 219, 197, 165, 150, 135
	loss of C16H24N2O2	$[C10H13O2]^+$	165.0916	1.8			
M3	O-Demethylation (to ring B)	$[M+H]^+$	441.2753	2.5	5.35	0.6	QqQ: 441, 303, 289, 260, 246
	loss of C9H12O2	$[C18H27N2O2]^+$	303.2073	0.4			QTrap: 441
	loss of C17H26N2O2	$[C9H11O2]^+$	151.0759	0.3			
M4	N-Demethylation	$[M+H]^+$	441.2753	0.4	5.56	40.3	QqQ: 455, 441, 303, 289, 260, 246, 165, 151, 150, 136
	loss of C9H12O2	$[C17H25N2O2]^+$	289.1916	0.1			
	loss of C10H15NO2	$[C16H22NO2]^+$	260.1651	0.9			QTrap: 441, 289, 260, 228, 220, 165, 150, 135
M5	2 × Demethylation (both to ring A or one to ring A and N-Demethylation)	$[M+H]^+$	427.2597	0.1	5.05	1.9	QqQ: 427, 165, 150
	loss of C15H22N2O2	$[C10H13O2]^+$	165.0916	2.5			QTrap: 427, 277, 260, 177, 165, 150, 135, 119, 91
M6	2 × Demethylation (both to ring A or one to ring A and N-Demethylation)	$[M+H]^+$	427.2597	1.1	5.20	0.2	QqQ: 427, 165, 150
	loss of C15H22N2O2	$[C10H13O2]^+$	165.0916	2.7			QTrap: 427
M7	2 × Demethylation	$[M+H]^+$	427.2597	1.3	5.27	0.1	
M8	3 × Demethylation	$[M+H]^+$	413.2440	0.0	3.72	0.1	
M9	Hydroxylation	$[M+H]^+$	471.2859	0.7	3.29	0.1	
M10	Hydroxylation/N-oxidation to C17H25N2O2 area	$[M+H]^+$	471.2859	2.5	3.82	0.2	QqQ: 471, 457, 439, 165, 150 QTrap: 471, 261, 218, 165, 150
M11	Hydroxylation/N-oxidation to C17H25N2O2 area	$[M+H]^+$	471.2859	0.6	3.98	0.1	QqQ: 471, 457, 165 QTrap: 471, 231, 165, 150
M12	Hydroxylation/N-oxidation	$[M+H]^+$	471.2859	0.4	4.24	0.1	
M13	Hydroxylation/N-oxidation	$[M+H]^+$	471.2859	0.6	4.35	0.1	
M14	Hydroxylation (to ring B or carbon next to it)	$[M+H]^+$	471.2859	−0.3	4.49	0.2	QTrap: 471, 291, 260, 248, 233, 181, 177, 166, 149, 136
	loss of C10H12O3	$[C17H27N2O2]^+$	291.2073	0.5			
	loss of C17H26N2O2	$[C10H13O3]^+$	181.0865	0.5			
M15	Hydroxylation/N-oxidation	$[M+H]^+$	471.2859	0.7	5.11	0.1	
M16	Hydroxylation (to ring B or carbon next to it)	$[M+H]^+$	471.2859	0.0	5.41	2.1	QqQ: 471, 303, 260, 181
	loss of C17H26N2O2	$[C10H13O3]^+$	181.0865	2.9			QTrap: 471, 453, 303, 291, 260, 248, 233, 219, 181, 166, 149
M17	2 × Hydroxylation (to C10H12O2 area)	$[M+H]^+$	487.2808	−1.0	4.52	0.4	QqQ: 487, 405, 303, 260
	loss of C9H12O4	$[C18H27N2O2]^+$	303.2073	0.2			
M18	3 × Hydroxylation/N-oxidation	$[M+H]^+$	503.2757	−2.2	4.02	0.1	
M19	3 × Hydroxylation/N-oxidation	$[M+H]^+$	503.2757	0.4	4.22	0.1	
M20	3 × Hydroxylation/N-oxidation	$[M+H]^+$	503.2757	−1.1	5.44	0.1	

DOI: 10.1002/rcm

RCM

M21	Hydroxylation to isopropyl + N-Demethylation	$[M+H]^+$	457.2702	0.3	3.80	0.3	QqQ: 457, 150
	loss of C3H7O	$[C23H31N2O4]^+$	399.2284	0.2			QTrap: 457, 399, 354, 323, 247, 220, 179, 165, 150, 135
	loss of C16H24N2O3	$[C10H13O2]^+$	165.0916	1.8			
M22	Methyl hydroxylation + Demethylation	$[M+H]^+$	457.2702	−0.6	3.94	0.1	
	loss of CH3OH	$[C25H33N2O4]^+$	425.2440	1.4			
	losses of CH3OH and CH2	$[C24H31N2O4]^+$	411.2284	0.5			
M23	Methyl hydroxylation + Demethylation (not in ring B)	$[M+H]^+$	457.2702	−0.5	4.03	0.1	QTrap: 457, 177, 165, 150
	loss of CH3OH	$[C25H33N2O4]^+$	425.2440	2.5			
M24	Hydroxylation + Demethylation to C17H25N2O2 area	$[M+H]^+$	457.2702	2.0	4.36	0.3	QqQ: 457, 443, 165, 150
	loss of C9H12O2	$[C17H25N2O3]^+$	305.1865	−0.2			QTrap: 457, 165
	loss of C16H24N2O3	$[C10H13O2]^+$	165.0916	1.5			
M25	Hydroxylation + Demethylation	$[M+H]^+$	457.2702	−1.3	4.64	0.1	
M26	Hydroxylation + Demethylation	$[M+H]^+$	457.2702	−1.7	4.74	0.1	
M27	Hydroxylation to isopropyl + O-Demethylation (to ring B)	$[M+H]^+$	457.2702	−0.3	5.30	1.4	
	loss of H2O	$[C26H35N2O4]^+$	439.2597	1.1			
	loss of C3H9O	$[C23H28N2O4]^+$	396.2049	1.8			
	losses of C3H9O and C9H12O2	$[C14H16N2O2]^+$	245.1290	0.8			
M28	Hydroxylation to C10H12O2 area + N-Demethylation	$[M+H]^+$	457.2702	1.3	5.37	1.1	QqQ: 457, 439, 260, 150
	loss of C16H24N2O2	$[C10H13O3]^+$	181.0865	3.3			QTrap: 457
M29	Hydroxylation + 2 × Demethylation	$[M+H]^+$	443.2546	4.4	3.62	0.1	
	loss of CH2O	$[C24H33N2O4]^+$	413.2440	1.6			
M30	Hydroxylation + 2 × Demethylation	$[M+H]^+$	443.2546	−0.2	3.84	0.1	
M31	Hydroxylation + 2 × Demethylation	$[M+H]^+$	443.2546	0.2	4.33	0.1	
M32	Hydroxylation + 2 × Demethylation	$[M+H]^+$	443.2546	−0.6	4.60	0.1	
M33	Hydroxylation + 2 × Demethylation	$[M+H]^+$	443.2546	0.2	4.68	0.1	
M34	N-Dealkylation by loss of C10H12O2	$[M+H]^+$	291.2073	0.2	3.24	32.9	QqQ: 291, 260, 165, 150, 96
	losses of C3H7 and CH2	$[C13H18N2O2]^+$	234.1368	0.1			QTrap: 291, 244, 233, 230, 217, 202, 187, 177, 165, 151, 150, 137
M35	N-Dealkylation + O-Demethylation	$[M+H]^+$	277.1916	0.3	2.38	0.7	
	loss of CH3NH2	$[C15H20NO2]^+$	246.1494	0.9			
	loss of C3H7	$[C13H18N2O2]^+$	234.1368	0.1			
M36	N-Dealkylation + O-Demethylation	$[M+H]^+$	277.1916	0.7	2.53	0.1	
M37	N-Dealkylation + N-Demethylation	$[M+H]^+$	277.1916	−0.3	3.16	5.0	QqQ: 277, 165
	loss of NH3	$[C16H22NO2]^+$	260.1651	1.0			
	loss of C3H7	$[C13H18N2O2]^+$	234.1368	0.3			
M38	N-Dealkylation + 2 × Demethylation	$[M+H]^+$	263.1760	−0.2	2.28	0.1	
M39	N-Dealkylation + Demethylation + Hydroxylation	$[M+H]^+$	293.1865	−0.3	2.08	0.1	
M40	N-Demethylation + Dehydrogenation	$[M+H]^+$	439.2597	2.6	4.88	0.8	QqQ: 439, 260
	loss of C9H10O2	$[C17H25N2O2]^+$	289.1916	0.9			
	loss of C10H13NO2	$[C16H22NO2]^+$	260.1651	0.5			
M41	Demethylation + Dehydrogenation	$[M+H]^+$	439.2597	1.0	5.45	0.2	
M42	Demethylation + Dehydrogenation	$[M+H]^+$	439.2597	3.4	5.53	0.1	
M43	Demethylation + 2 × Dehydrogenation	$[M+H]^+$	437.2440	0.3	5.46	0.2	
M44	2 × Demethylation + Dehydrogenation	$[M+H]^+$	425.2440	−0.2	3.57	0.1	
M45	2 × Demethylation + Dehydrogenation	$[M+H]^+$	425.2440	3.3	4.12	0.1	
M46	2 × Demethylation + Dehydrogenation	$[M+H]^+$	425.2440	3.2	4.31	0.1	
M47	2 × Demethylation + Dehydrogenation	$[M+H]^+$	425.2440	3.0	4.71	0.1	

(*Continues*)

DOI: 10.1002/rcm

Table 5. (Continued)

	Metabolite name	Ion	*m/z* Calc.	mDa TOF	RT (min)	%	Fragment ions from QqQ and QTrap
M48	Hydroxylation + Demethylation + Dehydrogenation	$[M+H]^+$	455.2546	0.3	3.77	0.1	
M49	Hydroxylation + Demethylation + Dehydrogenation	$[M+H]^+$	455.2546	0.8	4.67	0.1	
M50	Hydroxylation + Demethylation + Dehydrogenation to C17H25N2O2 area	$[M+H]^+$	455.2546	−0.4	5.94	0.4	QqQ: 455, 165, 150
	loss of C16H22N2O3	$[C10H13O2]^+$	165.0916	1.4			
M51	Hydroxylation + Demethylation + Hydrogenation	$[M+H]^+$	459.2859	0.7	4.11	0.2	
M52	Cleavage of C17H25N2O2 + Hydroxylation	$[M+H]^+$	183.1021	1.7	2.70	0.3	
M53	Glucuronide conjugation	$[M+H]^+$	631.3231	−1.0	5.70	0.1	QqQ: 631, 455 QTrap: 631
M54	O-Demethylation (to ring A) + Glucuronide conjugation	$[M+H]^+$	617.3074	−0.1	5.00	2.6	QqQ: 617, 603, 441, 439, 427, 165, 150
	loss of C6H8O6	$[C26H37N2O4]^+$	441.2753	2.1			QTrap: 617, 441, 289, 246, 165, 150
M55	O-Demethylation (to ring B) + Glucuronide conjugation	$[M+H]^+$	617.3074	1.7	5.17	0.7	QqQ: 617, 441, 260, 150 QTrap: 617, 441, 291, 260, 248, 151
M56	Demethylation + Glucuronide conjugation	$[M+H]^+$	617.3074	3.3	5.60	0.1	QqQ: 617, 441 QTrap: 617
	loss of CH2	$[C31H43N2O10]^+$	603.2918	2.7			
M57	2 × Demethylation + Glucuronide conjugation	$[M+H]^+$	603.2918	0.1	4.15	0.1	
M58	2 × Demethylation + Glucuronide conjugation	$[M+H]^+$	603.2918	−1.0	4.42	0.1	
M59	2 × Demethylation (both to ring A or one to ring A and N-Demethylation) + Glucuronide conjugation	$[M+H]^+$	603.2918	0.5	4.99	1.8	QqQ: 603, 441, 439, 427, 165, 150
	loss of C6H8O6	$[C25H35N2O4]^+$	427.2597	0.9			QTrap: 603, 427, 275, 233, 207, 165, 150
M60	Hydroxylation + Glucuronide conjugation	$[M+H]^+$	647.3180	3.8	5.62	0.5	QqQ: 647, 471, 455, 441, 260, 165, 150
	loss of CH2	$[C32H45N2O11]^+$	633.3023	−2.0			
	loss of C6H8O6	$[C27H39N2O5]^+$	471.2859	0.6			
M61	Hydroxylation + Demethylation + Glucuronide conjugation	$[M+H]^+$	633.3023	−1.2	2.62	0.1	
M62	Hydroxylation + Demethylation + Glucuronide conjugation	$[M+H]^+$	633.3023	1.2	4.48	0.1	
M63	Hydroxylation + Demethylation + Glucuronide conjugation	$[M+H]^+$	633.3023	−0.1	4.58	0.1	
M64	Hydroxylation + Demethylation + Glucuronide conjugation	$[M+H]^+$	633.3023	−0.8	5.05	0.1	
M65	Hydroxylation + Demethylation + Glucuronide conjugation	$[M+H]^+$	633.3023	0.1	5.19	0.1	QqQ: 633, 165, 150
M66	Hydroxylation + Demethylation + Glucuronide conjugation	$[M+H]^+$	633.3023	0.5	5.29	0.1	
M67	Hydroxylation + 2 × Demethylation + Glucuronide conjugation	$[M+H]^+$	619.2867	0.1	4.52	0.1	
M68	2 × Demethylation + Dehydrogenation + Glucuronide conjugation	$[M+H]^+$	601.2761	−1.4	3.90	0.1	
M69	N-Dealkylation + Demethylation + Glucuronide conjugation	$[M+H]^+$	453.2237	−0.8	2.16	0.1	

mDa = difference between calculated and obtained accurate mass

% = share of total combined metabolite peak areas from TOFMS data assuming similar MS response of the metabolites

DOI: 10.1002/rcm

RCM

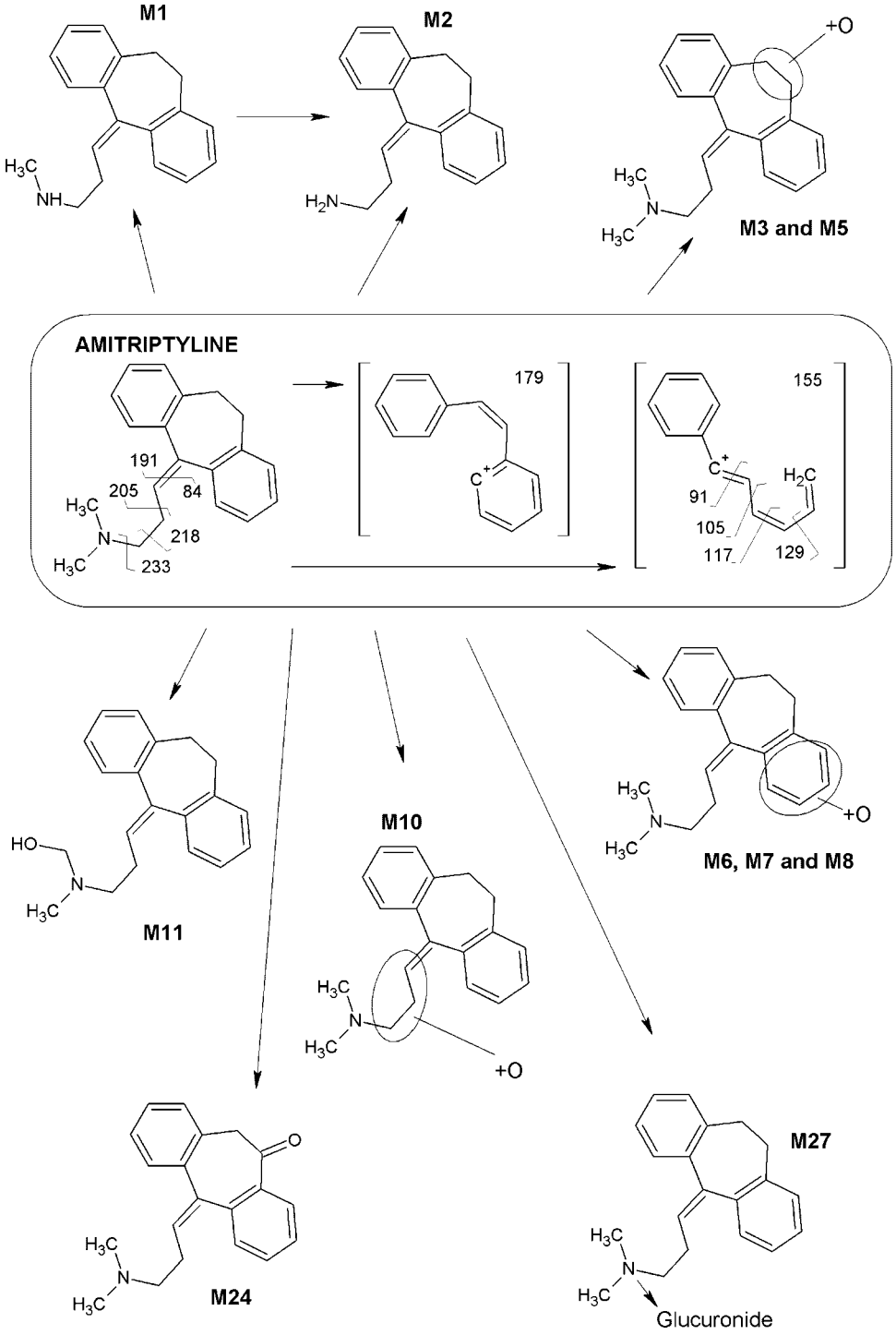

Figure 1. Proposed amitriptyline biotransformations and fragmentation.

TOFMS is about 15-fold in comparison to the other three instruments, with which an approximately similar S/N ratio was observed. It is however worth noticing that the signal from the QqQ instrument is strongly skewed and defined only by a couple of chromatographic data points, so that probably even a very slight decrease in concentration would have led to missing this metabolite. Moreover, the XIC from LTQ-Orbitrap data is created using the same 50 mDa window as that from TOFMS data, to observe some noise and to be able to calculate the S/N ratio. Use of a smaller XIC window size would have cut down the noise from both TOFMS and LTQ-Orbitrap data practically completely, making it more difficult to evaluate the S/N ratio. Thus, the sensitivity difference between TOFMS and the LTQ-Orbitrap is somewhat overestimated in this figure, but the data however shows a better sensitivity with TOFMS with respect to other tested MS instruments.

Identification of metabolites and proposed fragmentation pathways

Biotransformations for all found metabolites were tentatively identified with accurate mass obtained from TOFMS/

DOI: 10.1002/rcm

RCM

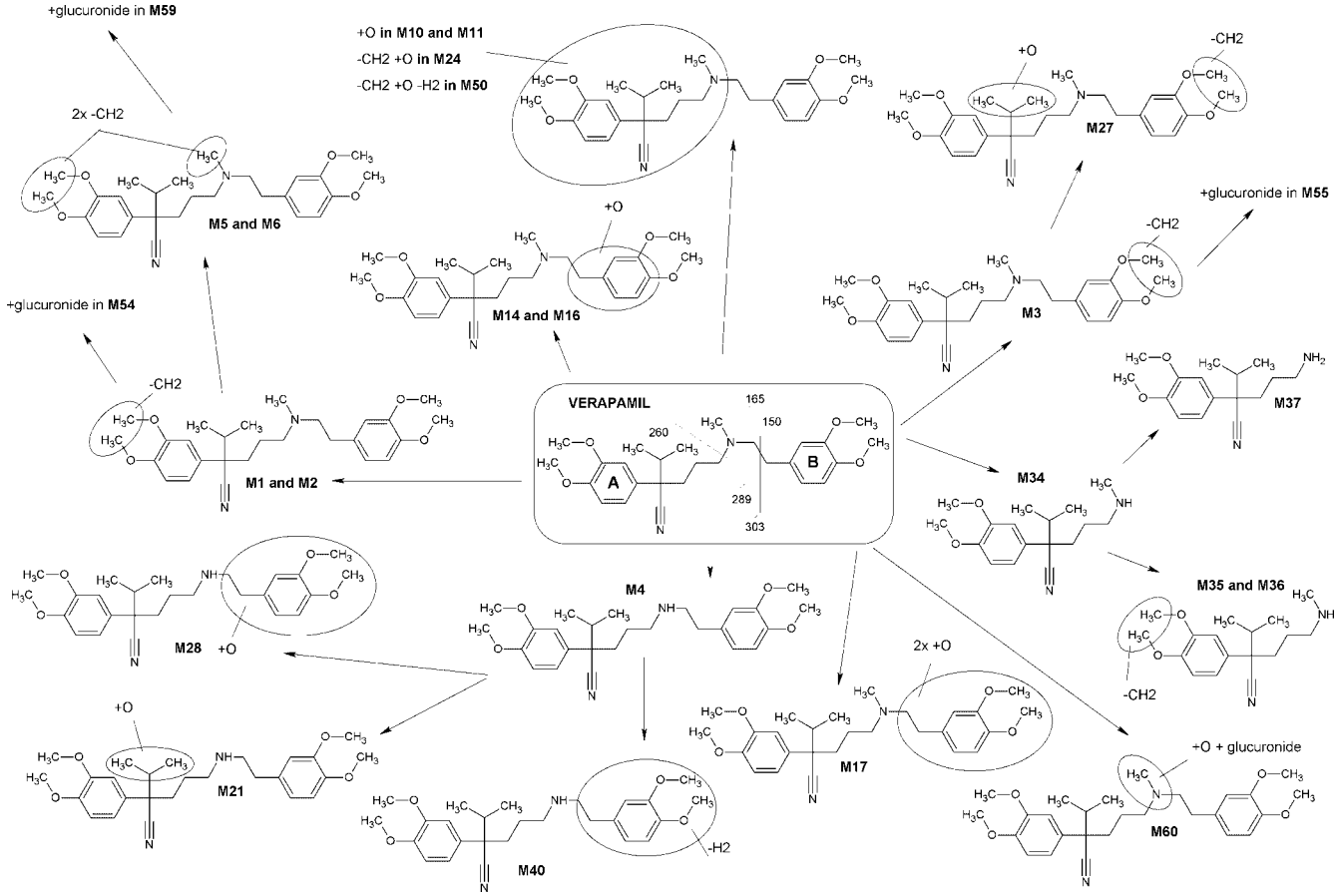

Figure 2. Proposed verapamil biotransformations and fragmentation.

LTQ-Orbitrap data, and accurate mass in-source fragment ion data from TOF experiments were used together with low-resolution fragment ion data obtained from QqQ, Q-Trap and LTQ-Orbitrap (for amitriptyline only) experiments to further elucidate the metabolite structures. All accurate mass and fragment ion data obtained for amitriptyline and verapamil are collected in Tables 4 and 5, respectively. Very good mass accuracies were obtained for all molecular ions and their in-source fragments detected with TOFMS, as in general the differences between calculated and measured *m/z* values were below 2 mDa.

For amitriptyline, the clear main metabolic route was N-demethylation (M1), which had about 65% share of the total combined metabolite LC/MS peak area (in TOFMS data). In addition, nine hydroxylated (or N-oxidized) metabolites (M3–M11) were the only metabolites formed via single biotransformation reaction only. After this, all other detected metabolites were formed as a combination of several biotransformation reactions, i.e. hydroxylations/N-oxidations, one or two N-demethylations, dehydrogenation, along with N- or O-glucuronide conjugations. Both mono- and di-demethylated M1 and M2 produced the same fragment ions as the parent molecule.

Of the hydroxyl metabolites M3–M11, in M3 and M5 the biotransformation sites were identified to the ethylene bridge between two aromatic rings, even though this will lead to some inconsistencies with regard to the fragment ion identification. The presence of very intense loss of water (*m/z* 276) points to the hydroxylation site being either in the ethylene bridge or in the C_2H_4 part of the side chain (non-aromatic or non-double-bond carbon), and the fragment ions at *m/z* 84 point to an unmodified side chain in both M3 and M5. Also the ions at *m/z* 216/215 and 153, being 2 or 3 mass units smaller than the corresponding ions with the parent, after loss of water from the hydroxylated fragment, point to the hydroxylation site being in this ethylene bridge area. These two ethylene bridge hydroxylations are indeed well known in amitriptyline metabolism.[29] The contradiction in biotransformation site elucidation is however raised by the M3 and M5 fragment ions at *m/z* 205, 191, and 203, which are the same as the parent, and, if formed via an identical fragmentation pathway (see Fig. 1), this would point to the biotransformation site being the side chain. If figuring out the fragmentation map for the first two of these, it can be suggested that cleavages of water and unmodified side chain in M3 and M5 can lead to fragment ions at *m/z* 205 and 191 that are isobaric to amitriptyline fragments, even though having slightly different structure. The ion at *m/z* 203 is however more problematic, as the only identification we could come up for that is loss of H_2 from *m/z* 205, meaning that in the case of ethylene bridge-hydroxylated metabolites the ion at *m/z* 203 should be preceded by an ion at *m/z* 221 (*m/z* 205+16), that was not detected here. The ion at *m/z* 231 may be formed from both possible abovementioned hydroxylation sites as well, and do not elucidate the biotransformation site more exactly. One additional suggestion to the ethylene

DOI: 10.1002/rcm

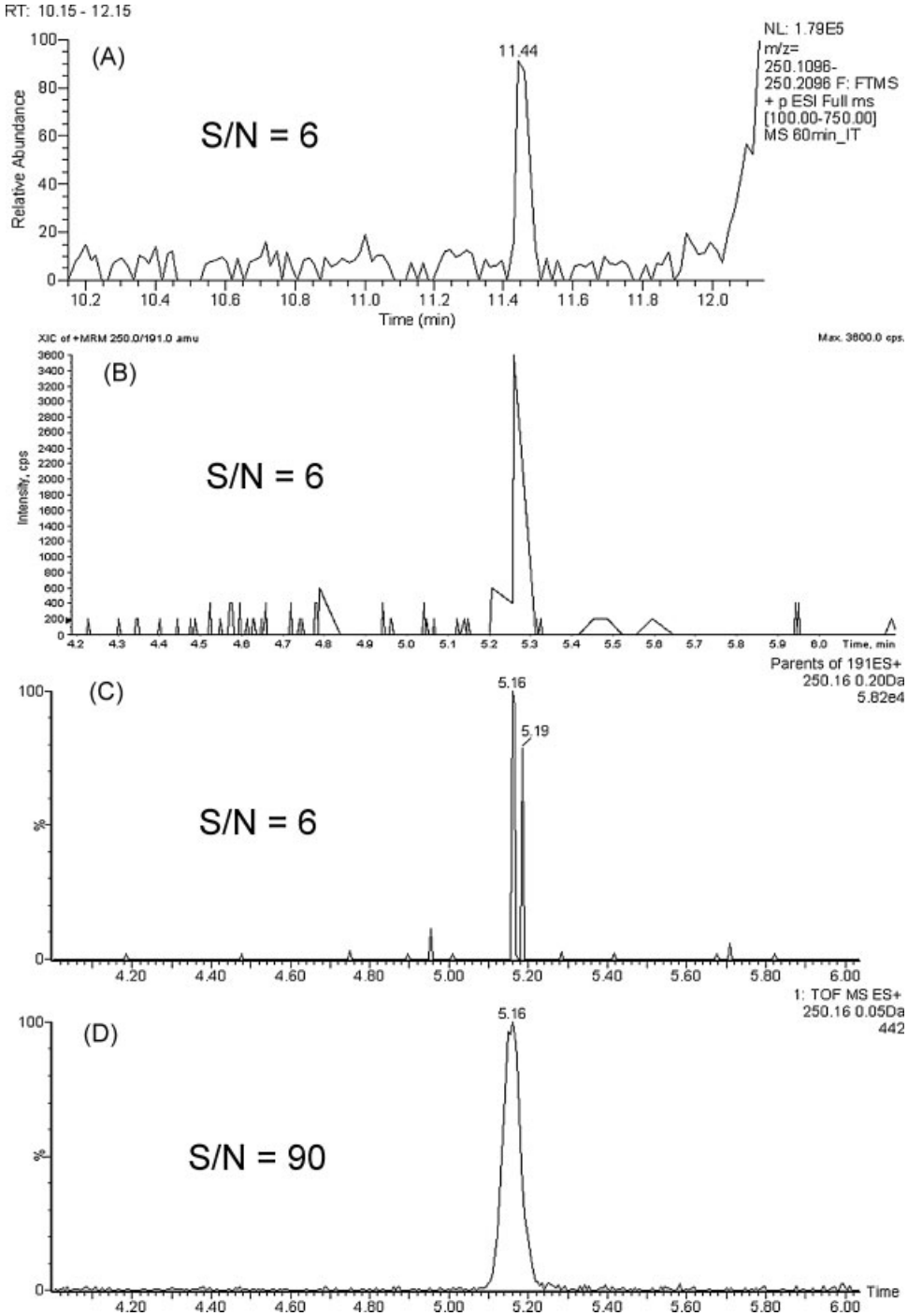

Figure 3. Extracted ion chromatograms of di-demethylated M2 of amitriptyline from LTQ-Orbitrap (A), Q-Trap (B), QqQ (C), and TOF (D) data illustrating the detection sensitivity of different MS instruments in this study.

bridge as a hydroxylation site is M24 (see below), with clearer identification of the formation of an oxo to ethylene bridge area (possibly by further dehydrogenation of M3 or M5). Despite this somewhat ambiguous fragment ion identification, more experiments were not conducted, as the main issue of the work was to compare the instrumentation in one lab visit only, and not the actual comprehensive identification of amitriptyline metabolism.

Aromatic hydroxylation in M6 was identified with fragment ions +16 mass units compared to fragment ions of the precursor. In M7 the hydroxylation was located to the three-ring area based on fragment ions *m/z* 207 (*m/z* 191 + 16) and 84, and the fragment ion at *m/z* 121 (*m/z* 105 + 16) narrows the hydroxylation site to an aromatic ring. In M8 the fragment ions at *m/z* 207 (*m/z* 191 + 16), 107 (*m/z* 91 + 16) and 91 suggest also aromatic hydroxylation. In M10 the fragment ion at *m/z* 249, by loss of C_2H_7N, and the fragment ion at *m/z* 205, pinpoint the hydroxylation site to the three-carbon area between the nitrogen atom and the central ring, and the lack of a fragment ion by loss of water suggests that the site may

DOI: 10.1002/rcm

most probably be the carbon next to the ring. This however requires that the proton/hydroxyl attached to this carbon is cleaved in the reaction forming the ion at *m/z* 205. The cleavage of CH_2O to produce a fragment ion at *m/z* 264 was used to identify M11 as methylhydroxylation instead of N-oxidation. For metabolites M12–M23 and M25–M26, no fragment ion data (or only a few less informative fragments) was obtained due to their low abundance, and they were identified based only on the accurate mass data for the molecular ion. In M24, the formation of an oxo group to the ethylene bridge after hydroxylation and dehydrogenation reactions were suggested by the presence of fragment ions +14 mass units compared to the precursor (*m/z* 232, 219 and 205 with respect to *m/z* 218, 205 and 191). Also the fragment ion at *m/z* 84 suggests the cleavage of an unmodified side chain in M24. The fragment ion at *m/z* 191 of M24 was then suggested to be formed via cleavage of the side chain and loss of the keto-oxygen as H_2O. M27 was identified as an N-glucuronide conjugate, as no other site for conjugation is available. M28 was formed by hydroxylation and further glucuronide conjugation. The observed fragment ions did not reveal the site for the hydroxylation nor the conjugation. The proposed biotransformation reactions and their sites (for amitriptyline metabolites to which fragment ion data was obtained) are shown in Fig. 1.

For verapamil, the main metabolic routes were N-demethylation (M4) and N-dealkylation by loss of $C_{10}H_{12}O_2$ (M34), having about 40% and 33% share of the total combined metabolite peak area (from LC/TOFMS data), respectively. Metabolites M1–M8 were formed via one or more N- and/or O-demethylations, M9–M20 via one to three hydroxylations/N-oxidations, M34 via N-dealkylation, and all the remaining metabolites were formed via combinations of these presented reactions or additional dehydrogenation or hydrogenation reactions, along with N- or O-glucuronide conjugations. For the demethylated metabolites, M1, M2 and M4, the presence of fragment ions at *m/z* 165 and 150, corresponding to unmodified ring B, suggests that the biotransformations have occurred as O-demethylations in ring A and/or as N-demethylation. Of these M4 with the fragment ion at *m/z* 260 was identified as N-demethylation. Similarly, the fragment ion at *m/z* 165 observed with M5 and M6 suggests that ring B is unmodified, and thus that demethylations have occurred either both in ring A or one in ring A and the other being N-demethylation. Of the hydroxy/N-oxide metabolites M9–M16, M10 and M11 had fragment ions at *m/z* 165 and 150, pinpointing the biotransformation sites to the $C_{17}H_{25}N_2O_2$ area. The fragment ions at *m/z* 181 and 166 for M14 and M16 show that the hydroxylation site is in either ring B or the carbon atom next to it. In M17, dihydroxylation is suggested to be located in the $C_{10}H_{12}O_2$ area, based on the fragment ions at *m/z* 303 and 260. In M21 the cleavage of C_3H_7O, resulting in the fragment ion at *m/z* 399, pinpoints the hydroxylation to the isopropyl group, and the fragment ion at *m/z* 220 shows that the demethylation is located on the nitrogen atom. In M22 and M23 the fragment ion by cleavage of methanol suggests that the hydroxylations have occurred to the methyl group. In M24 the hydroxylation or N-oxidation and demethylation were pinpointed to the $C_{17}H_{25}N_2O_2$ area by the presence of the fragment ion at *m/z* 165. In M27 the fragment ions at *m/z* 396 and 245 locate the hydroxylation to isopropyl and the O-demethylation to ring B. In M28, fragment ions at *m/z* 181 and 260 suggest a hydroxylation to $C_{10}H_{12}O_2$ area and an N-demethylation. Metabolites M35–M39 were further metabolites of N-dealkylated M34. The fragment ion at *m/z* 246 for M35 and at *m/z* 260 for M37 differentiate the O- and N-demethylations. M40 and M50 were the only dehydrogenated verapamil metabolites for which fragment ion data was obtained. The fragment ion at *m/z* 260 along with the ion at *m/z* 289 (*m/z* 303 – 14) resolved the N-demethylation in M40. For M50, the fragment ion at *m/z* 165 shows that the ring B area is intact. Metabolites from M53 to M69 were identified as glucuronide conjugates. For M54 the fragment ions at *m/z* 165 (unmodified ring B), 289 (*m/z* 303 – 14) and 246 (*m/z* 260 – 14) identify the O-demethylation to ring A. For M55, the fragment ions at *m/z* 291 and 260, together with an ion at *m/z* 151 (*m/z* 165 – 14) locates the O-demethylation to ring B. For M59, the two demethylations were either both in ring A, or the other is N-demethylation. For M60, the fragment ions at *m/z* 260 and 165 suggest the additional oxygen atom to be either N-methylhydroxylation or N-oxidation, which is followed by further glucuronide conjugation. The proposed biotransformation reactions and their sites (for the verapamil metabolites for which fragment ion data was obtained) are shown in Fig. 2.

As the main objective of this comparison is to test the feasibility of different MS instruments in metabolite screening and evaluate the data obtained with the instruments, the identification of the metabolites and biotransformation sites was not complete. Thus, we did not try to confirm the biotransformation sites by other available methods, nor were any of the identified metabolites purchased or synthesized.

Aspects for obtained structural data

Accurate mass data was obtained for all of the identified metabolites with TOF and LTQ-Orbitrap instruments, and in general the measured masses differed from the calculated monoisotopic masses by less than 2 mDa. For some of the minor metabolites or fragment ions with very low abundances slightly poorer mass accuracies were obtained. As expected, the overall mass accuracy for molecular ions was slightly better in LTQ-Orbitrap data (survey scan) in comparison to TOFMS data, but also the TOFMS mass accuracy was good enough and did not leave more than one possible identification of molecular formula in any case, i.e. no real meaningful difference was observed between the instruments. Moreover, it is worth keeping in mind that recent advances in TOF mass spectrometers, i.e. at least two instrument vendors now market Q-TOFs capable of mass resolution of 40 000 (FWHM) and very high mass accuracy, have narrowed the gap in comparison to the LTQ-Orbitrap.

The quality and quantity of the obtained fragment ion data varied between different MS instruments, as expected, and all of them had strengths and weaknesses. The lowest quantity of fragment ions was obtained with TOF, being the only instrument lacking a collision cell. Even though quite good elucidation of the biotransformation sites for the main metabolites was observed also from TOFMS data, a number of fragment ions important for more accurate structural

DOI: 10.1002/rcm

elucidation were missed in the TOFMS approach with respect especially to the Q-Trap. This disadvantage would have naturally been overcome by using the Q-TOF instrument instead of plain TOF, but that was not available for this study. Moreover, this might have decreased the TOF detection sensitivity due to the lower overall ion transmission to the detector in the Q-TOF with respect to TOF. The obvious strength of TOFMS is that accurate mass data was obtained also for fragment ions, which was not the case with the LTQ-Orbitrap, with which the use of high-resolution detection mode for fragment ions would have led to absolutely too long scan cycle times. The accurate mass information for fragment ions is much emphasized in structural elucidation, as often the fragment ion identifications may be easily erroneous without this data.[32] With QqQ and the Q-Trap we obtained pretty much equal amounts of fragment ion data. However, we used a high number of PI and NL functions with the QqQ, leading to several LC/MS runs, whereas the Q-Trap was used only in one run per sample approaches, meaning that if more runs had been used to utilize the ion trap feature of the Q-Trap, the number of fragment ions obtained could have easily been even higher. This is naturally the case also if the ion trap feature of the LTQ-Orbitrap would have been used more with additional LC/MS runs. Even though providing high amounts of fragment ion data, the serious drawback of QqQ as well as the Q-Trap instrument was naturally the inability to produce accurate mass data, which has a very important role in confirming the changes in molecular formulae due to biotransformation reactions.

With LTQ-Orbitrap experiments high-resolution full scan was used as a survey scan in conjunction with data-dependent acquisition of low-resolution MS/MS spectra for the two most abundant ions. With this kind of setup a total cycle time of around 1 s was obtained, which produced adequate structural information for the main metabolites in this study. The amount and quality of the MS/MS data obtained with the LTQ-Orbitrap for the minor metabolites was however rather poor, as the measured MS/MS data was mainly produced by ions from matrix constituents, despite the use of a comprehensive background ion exclusion list. This disadvantage could have been overcome by a more thorough setup of the inclusion list for expected metabolite ions, so that those ions are chosen for CID when present, even if more abundant ions were detected in the same survey scan. Also an approach similar to the one described by Ruan *et al*.,[13] i.e. using mass resolution of 7500 for MS/MS events, was tested but this resulted in a scan cycle exceeding 2 s that was clearly too long and led to missing metabolites due to inadequately defined chromatographic peak shapes and decreased sensitivity, even though a slower chromatographic method with broader peak widths was used in LTQ-Orbitrap experiments with respect to other instruments. Despite this disadvantage some approaches with high mass resolution for fragment ion data acquisition, suffering from slow data acquisition rates, have been described. For example, a total duty cycle of even 5.6 s has been reported.[12] Recently, Li *et al*.[33] described an two-injection approach, where the other injection with precursor-specific MS/MS experiments were conducted after interpretation of the data from the first injection, to overcome the interference of matrix constituents in fragment ion data acquisition. Moreover, they showed that with proper settings also the data acquisition speed of the LTQ-Orbitrap could be improved, even though their data still contained 0.3 min broad chromatographic peaks with long chromatographic run times.

Aspects for the workload of different approaches

The time consumption for the described analyses was clearly the lowest when using the TOF instrument. With this approach only one injection/sample is needed and all of the expected as well as all of the unexpected metabolites are detected within a single run without any need for metabolite prediction for certain special metabolites, or elucidation of parent compound fragmentation pathways before analysis, thus being very applicable for high-throughput analysis. Based on the high amount of data from a single run, it is laborious to mine metabolites from the total ion current data, but fortunately very good software exists to ease the process. In most cases, and to guarantee the results – practically always, there is a need for manual expert evaluation and confirmation of the software-produced results, and therefore the whole process cannot be totally automated, especially with regard to the unexpected metabolites. With this approach the total workload, after finding suitable LC/MS conditions (gradient strength and pH in chromatography), is typically about 30 min of instrument time and 1–4 h of data processing per compound/species, depending on the number of metabolites and on the complicity of the interpretation of the fragment ion data. However, some of the recently described software may also take care of the fragment ion data interpretation, especially if a Q-TOF instrument is used.[27]

The experiments with the triple quadrupole consumed a lot of instrument time and also a high volume of sample. Amitriptyline produced ten abundant fragment ions under CID and therefore ten different PI scan and 11 different NL scan functions were acquired, thus 21 injections for each of blank, 0 min sample and 60 min sample were conducted. Twenty different traces were processed so that over 1000 extracted ion chromatograms were evaluated manually in order to mine the data for metabolites. The processing of verapamil data also involved a manual evaluation of over 1000 ion chromatograms as 42 traces were checked from nine scan functions within three samples. In total the acquisition of the data was conducted overnight and the metabolites were mined manually in a time frame of a few working days.

The workload of the Q-Trap experiments lies somewhere in between those of TOF and QqQ experiments. With the used SRM-ER-EPI and EMS-ER-EPI approaches the most laborious part is the prediction of possible biotransformations and thus the generation of predicted SRM/MRM reactions, even though the construction of compound-specific predicted SRM-IDA methods can also be automated by using Applied Biosystems/MDS SCIEX LightSight software.

In the case of the LTQ-Orbitrap experiments with the approach where only low-resolution MS/MS was performed, the workload of the acquisitions themselves is also

DOI: 10.1002/rcm

low – as only one injection per sample was used. Due to slow data acquisition rate about twice as many runs were needed in comparison to other instruments. In data processing, times quite similar to TOFMS would be expected, as a similar type of software-aided data processing was used. Because of our greater experience in using the MetaboLynx software (Waters, for TOF) with respect to MetWorks (Thermo-Scientific, for LTQ-Orbitrap), we wanted to avoid differences in results due to this, and used the TOFMS-detected metabolites as a list of expected metabolites when going through the LTQ-Orbitrap data.

Comparison with literature data and possible alternative screening methods

For amitriptyline, all the known main metabolites, and also most of the minor known metabolites,[29] were detected and tentatively identified by their accurate masses and fragment ion data. Many of the metabolites were of very low abundance and no fragment ion data was obtained for them with any of the used MS approaches. Therefore, the comparison of metabolites detected here with earlier reported amitriptyline metabolites is quite rough, e.g. with respect to biotransformation sites that remained unclear in many cases. Recently, a study of verapamil metabolism conducted with a newer and more sensitive version of the Q-Trap mass spectrometer (AB SCIEX QTRAP 5500) was reported, leading to a total of 35 detected verapamil metabolites from a fresh rat hepatocyte incubation spiked into rat bile.[30] That study used a two-injection methodology (predicted SRM using LightSight software and dual precursor and neutral loss survey scan) with 158 predicted SRM reactions generated from one parent compound fragmentation reaction (m/z 455 > 165). This shows that even the use of a very high number of predicted SRM reactions with the Q-Trap did not lead to as high a hit rate as in the TOFMS-based approach used here, but naturally it must be noted that also the used enzyme source was different (rat hepatocytes). In our own other recent study with a clearly less sensitive older generation TOF instrument than the one used in this study, the number of detected metabolites was higher with rat liver microsomal incubation in comparison to human liver microsomal incubation (8 vs. 7).[31]

With TOFMS we also tested a different approach where the fragment ion data was obtained with two injections of the sample, separating the acquisition of low and high aperture voltage data with 150 ms scan time into two separate runs. This data was then evaluated against a single injection protocol with two parallel scan functions with 100 ms scan time. The peak areas for abundant main metabolites in extracted ion chromatograms with two parallel functions were about 50–80% of the peak areas when using only one function with longer scan time. For peaks of very low abundance (S/N ratio around 10 or less) the relative size of peaks in the two data function run were about 80–100% of those in separate one function runs, leading thus to an equal number of metabolite hits regardless of the approach used (data not shown). If yet alternative TOFMS-based approaches are searched, in addition to earlier mentioned latest generation very high resolution Q-TOF instruments, a use of the ion mobility feature must be mentioned, as described in metabolite profiling recently by Chan *et al*.[34]

In addition to the used approaches in Q-Trap experiments, the use of PI/NL scan functions can be used as a survey scan to trigger the acquisition of EPI spectra, as mentioned earlier. Also recently, yet one more alternative Q-Trap approach was introduced and applied to drug metabolite screening, utilizing monitoring of multiple predicted metabolite ions (MIM) in both quadrupoles with minimized fragmentation, and using it to trigger the acquisition of EPI spectra.[22,35] Selectivity of this methodology was similar to that of the SRM approach, and the sensitivity to obtain MS/MS data was improved in comparison to full scan approaches.

CONCLUSIONS

The time-of-flight mass spectrometer with high scanning sensitivity and rapid data acquisition speed was shown to have a superior performance over the other instrument types used here in early phase 'one lab visit only' metabolite profiling. The very high wide-mass range detection sensitivity allows easy simultaneous detection of both expected and unexpected metabolites in a single run, acquiring also fragment ion data at the same time. Moreover, the approach does not require any metabolite prediction or pre-adjusted detection reactions or changes in settings between different test compounds (except parameters with respect to ionisation properties), which was the case also when the LTQ-Orbitrap mass spectrometer was used in the analyses.

Both TOF and LTQ-Orbitrap instruments showed adequate mass accuracies to elucidate the change in molecular formula by metabolism, even though the mass accuracy of the LTQ-Orbitrap was slightly better. The drawback of the LTQ-Orbitrap with respect to TOFMS was its low data acquisition rate, because much longer LC/MS run times with poorer chromatographic resolution had to be used. In addition, the LTQ-Orbitrap was shown to have lower detection sensitivity in full scan-type analysis, which led to false negatives for many metabolites that the TOFMS approach was able to find. Considering the fragment ion data, the LTQ-Orbitrap was able to produce a higher number of different fragment ions in comparison to the TOFMS approach, but due to its low data acquisition speed the low-resolution mode had to be used to acquire the fragment ion data, and thus accurate masses were not obtained for them. This in turn suggests that the more evident strengths of the LTQ-Orbitrap instrument lie in the later phases of drug development studies, where the more accurate structural elucidation has an increased value, and time used per sample is less critical, meaning that the LTQ-Orbitrap can be used to acquire several LC/MS runs for one sample (or even one metabolite) with high-resolution MS/MS settings and even MS^n data.

The approaches used here with the Q-Trap and triple quadrupole mass spectrometers produced the highest amount of fragment ion data for structural elucidation, but the low sensitivity and very high time consumption with the triple quadrupole instrument made the approach very laborious, being neither time- nor cost-effective, and also provided the lowest number of detected metabolites. Also

DOI: 10.1002/rcm

the SRM/EPI approach with the Q-Trap instrument required laborious prediction of metabolites and their SRM reactions, and even with careful selection of these reactions a number of unexpected metabolites were missed.

Acknowledgements

The expert technical assistance of Dr. Yue Xuan from ThermoFisher Scientific is gratefully acknowledged for the LTQ-Orbitrap measurements. We are also grateful to Mrs Katri Sunnari and Mrs Birgitta Paldanius for technical assistance.

REFERENCES

1. Pelkonen O, Turpeinen M, Uusitalo J, Rautio A, Raunio H. *Basic Clin. Pharmacol. Toxicol.* 2005; **96**: 167.
2. Coecke S, Ahr H, Blaauboer BJ, Bremer S, Casati S, Castell J, Combes R, Corvi R, Crespi CL, Cunningham ML, Elaut G, Eletti B, Freidig A, Gennari A, Ghersi-Egea JF, Guillouzo A, Hartung T, Hoet P, Ingelman-Sundberg M, Munn S, Janssens W, Ladstetter B, Leahy D, Long A, Meneguz A, Monshouwer M, Morath S, Nagelkerke F, Pelkonen O, Ponti J, Prieto P, Richert L, Sabbioni E, Schaack B, Steiling W, Testai E, Vericat JA, Worth A. *Altern. Lab Anim.* 2006; **34**: 49.
3. Leclercq L, Cuyckens F, Mannens GSJ, de Vries R, Timmerman P, Evans DC. *Chem. Res. Toxicol.* 2009; **22**: 280.
4. Walker D, Brady J, Dalvie D, Davis J, Dowty M, Duncan JN, Nedderman A, Obach RS, Wright P. *Chem. Res. Toxicol.* 2009; **22**: 1653.
5. FDA Guidance for Industry. *Safety Testing of Drug Metabolites*, 2008. Available: http://www.fda.gov/downloads/Drugs/GuidanceComplianceRegulatoryInformation/GGuidance/ucm079266.pdf.
6. Tolonen A, Turpeinen M, Pelkonen O. *Drug Discov. Today* 2009; **14**: 120.
7. Tiller PR, Yu S, Castro-Perez J, Fillgrove KL, Baillie TA. *Rapid Commun. Mass Spectrom.* 2008; **22**: 1053.
8. Mortishire-Smith RJ, O'Connor D, Castro-Perez J, Kirby J. *Rapid Commun. Mass Spectrom.* 2005; **19**: 2659.
9. Cuyckens F, Hurkmans R, Castro-Perez J, Leclercq L, Mortishire-Smith RJ. *Rapid Commun. Mass Spectrom.* 2009; **23**: 327.
10. Wrona M, Mauriala T, Bateman KP, Mortishire-Smith RJ, O'Connor D. *Rapid Commun. Mass Spectrom.* 2005; **19**: 2597.
11. Hu Q, Noll RJ, Li H, Makarov A, Hardman M, Cooks RG. *J. Mass Spectrom.* 2005; **40**: 430.
12. Lim H-K, Chen J, Sensenhauser C, Cook K, Subrahmanyam V. *Rapid Commun. Mass Spectrom.* 2007; **21**: 1821.
13. Ruan Q, Peterman S, Szewc MA, Ma L, Cui D, Humphreys WG, Zhu M. *J. Mass Spectrom.* 2008; **43**: 251.
14. Liu DQ, Hop CECA. *J. Pharm. Biomed. Anal.* 2005; **37**: 1.
15. Hakala KS, Kostiainen R, Ketola RA. *Rapid Commun. Mass Spectrom.* 2006; **20**: 2081.
16. Prakash C, Soliman V. *Drug Metab. Dispos.* 1997; **25**: 1288.
17. Hager JW. *Rapid Commun. Mass Spectrom.* 2002; **16**: 512.
18. Hopfgartner G, Husser C, Zell M. *J. Mass Spectrom.* 2003; **38**: 138.
19. Hopfgartner G, Varesio E, Tschäppät V, Grivet C, Bourgogne E, Leuthold LA. *J. Mass Spectrom.* 2004; **39**: 845.
20. Li AC, Alton D, Bryant MS, Shou WZ. *Rapid Commun. Mass Spectrom.* 2005; **19**: 1943.
21. Li AC, Shou WZ, Mai TT, Jiang X. *Rapid Commun. Mass Spectrom.* 2007; **21**: 4001.
22. Yao M, Ma L, Duchoslav E, Zhu M. *Rapid Commun. Mass Spectrom.* 2009; **23**: 1683.
23. Xia Y-Q, Miller JD, Bakhtiar R, Franklin RB, Liu DQ. *Rapid Commun. Mass Spectrom.* 2003; **17**: 1137.
24. Anari MR, Sanchez RI, Bakhtiar R, Franklin RB, Baillie TA. *Anal. Chem.* 2004; **76**: 823.
25. Zhang H, Zhang D, Ray K, Zhu M. *J. Mass Spectrom.* 2009; **44**: 999.
26. Pelander A, Tyrkkö E, Ojanperä I. *Rapid Commun. Mass Spectrom.* 2009; **23**: 506.
27. Leclercq L, Mortishire-Smith RJ, Huisman M, Cuyckens F, Hartshorn MJ, Hill A. *Rapid Commun. Mass Spectrom.* 2009; **23**: 39.
28. Walles M, Thum T, Levsen K, Borlak J. *J. Chromatogr. B* 2003; **798**: 265.
29. Breyer-Pfaff U. *Drug Metab. Rev.* 2004; **36**: 723.
30. Liu H-F, Jones E. Applied Biosystems Technical Note: Breakthrough *in vivo* metabolite analysis using the AB Sciex QTRAP 5500 System and Predictive MRM. September 2009; 16.
31. Pelkonen O, Tolonen A, Rousu T, Tursas L, Turpeinen M, Hokkanen J, Uusitalo J, Bouvier d'Yvoire M, Coecke S. *ALTEX* 2009; **3**: 214.
32. Hill AW, Mortishire-Smith RJ. *Rapid Commun. Mass Spectrom.* 2005; **19**: 3111.
33. Li AC, Ding J, Jiang X, Denissen J. *Rapid Commun. Mass Spectrom.* 2009; **23**: 3003.
34. Chan ECY, New LS, Yap CW, Goh LT. *Rapid Commun. Mass Spectrom.* 2009; **23**: 384.
35. Yao M, Ma L, Humphreys WG, Zhu M. *J. Mass Spectrom.* 2008; **43**: 1364.

DOI: 10.1002/rcm